Seismic Reliability Analysis of NPP's Nonstructural Components using Surrogate Models

Jieun Hur
Visiting Assistant Professor, Dept. of Civil, Environment and Geodetic Engineering, The Ohio State University, Columbus, OH, U.S.A.

Zeyu Wang
Graduate Student, Dept. of Civil, Environment and Geodetic Engineering, The Ohio State University, Columbus, OH, U.S.A.

Abdollah Shafieezadeh
Associate Professor, Dept. of Civil, Environment and Geodetic Engineering, The Ohio State University, Columbus, OH, U.S.A.

Minkyu Kim
Principal Researcher, Korea Atomic Energy Research Institute, Daejeon, South Korea

ABSTRACT: This study evaluates the accuracy and computational efficiency of seismic probabilistic risk assessment (SPRA) using a new surrogate model-based reliability analysis and compares the results with the conventional Monte Carle Simulation (MCS) method. The newly developed Kriging-based reliability analysis approach, called REAK, is in the class of Adaptive Kriging-based MCS (AK-MCS) methods, but with the ability to estimate error in failure probability estimates, which is used as the stopping criterion in the reliability analysis. It is shown that REAK can reliably capture the failure probability of nonstructural components located in buildings of nuclear power plants, however, with significantly smaller number of simulations compared to MCS. Results also indicate that the probability of acceleration of nonstructural components in the first floor exceeding that on the second floor is small but not zero, indicating that it cannot be neglected as commonly done in current risk analysis procedures.

1. INTORDUCTION

Seismic probabilistic risk assessment (SPRA) is a methodology used to perform safety analysis of nuclear power plants (NPPs) subjected to seismic hazards. In NPPs, various types of nonstructural components are systemically connected to support the safe operations of the power plants. Among nonstructural components, electrical equipment is one of the essential components of the system. Not only their physical damage, but also their operational failure can lead to serious malfunctions of NPPs with high safety risk implications during earthquakes. However, in order to evaluate the seismic performance of these components, a large number of simulations and seismic analyses are required to adequately capture uncertainties, as the failure probability of electrical equipment is often small.

This study proposes surrogate models for evaluating seismic reliability of nonstructural components in an auxiliary building of a hypothetical NPP. The seismic performance of nonstructural components located at different places of the auxiliary building is estimated, and their physical and operational failures are evaluated under strong ground motion histories. The study uses a novel surrogate model-based reliability analysis called REAK to efficiently and accurately estimate the failure probabilities. REAK, which is developed by the authors, is in the class of Adaptive Kriging-based Monte Carle Simulation (AK-MCS) methods, but with the ability to estimate error in failure probability

estimates, which is used as the stopping criterion in the analyses. This approach is used to analyze the failure probability of nonstructural components in a two story building for a high intensity ground motion record. Therefore, it is expected that the probability of failure of equipment installed on the floor of the first (E1) and second (E2) stories of the building will be high, and rather easy to estimate. In addition to failure probabilities, we used MSC and REAK to estimate the likelihood of the acceleration of E1 exceeding E2, which is expected to be a rare event. This allows evaluation of the performance of REAK with respect to MCS in terms of accuracy and computational efficiency.

2. MODEL DESCRIPTION

2.1. Structural and Nonstructural Component Models in NPPs

This study involves failure probability assessment of essentially identical equipment at two levels of a building in a hypothetical nuclear power plant (NPP) subjected to seismic shakings. To validate the result of surrogate models, the conventional Monte Carlo simulations are performed with a large number of samples generated using Latin Hypercube Sampling (LHS) technique. Based on the simulation result, the failure probability of the equipment is evaluated at each of the two levels, and the joint failure probability is computed and compared with the analysis result by the surrogate model. For the building structure, a lumped-mass stick model is used and a ground motion history is applied in the horizontal direction. From the analysis, the seismic response of the components are evaluated and compared to corresponding limit-states to estimate the failure probability of the equipment. Figure 1 illustrates: (a) the simplified model of a two-story auxiliary building in a pseudo-plant, (b) a stick model used for the characterization of the building with non-structural components E1 and E2 affixed to the first and second floors of the building, and (c) the nonstructural components restrained on floors. In this study, the fundamental frequency of the auxiliary building is assumed as 7.0 Hz, based on analyses performed by Kitada (1999) who assessed the fundamental frequencies of a two story auxiliary building lie in the range of 6 to 8 Hz.

Nonstructural components E1 and E2 represent essential electrical equipment in an auxiliary building of a nuclear power plant. Based on the literature on the fragility functions of electrical equipment using shaking table tests (Ellingwood, 1998; NUREG, 1987), the capacity function of a DC battery rack is assumed as a lognormal distribution with a median failure value of 1.01 g with β_R = 0.28, and β_U = 0.63. It is assumed that one type of electrical equipment is used at all floors and their capacity are identical. Electrical equipment can have various limit states representing operational failure as well as physical damage. It is common that slender electrical equipment such as electrical cabinets or racks reach the operational failure earlier than physical (structural) failure such as falling apart or tipping over (Hur, 2012). For this study, the limit state function is randomly generated based on the lognormal distribution of the DC battery rack as shown in Table 1.

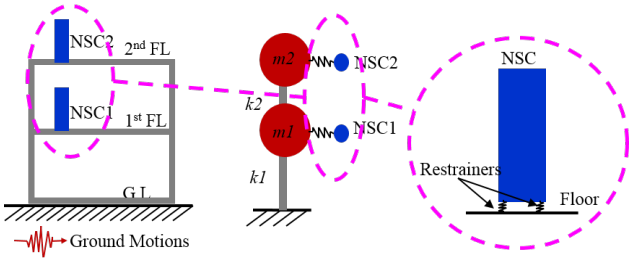

Figure 1: Simplified Models for a Building in a NPP

Based on the assumption that the mean value of the fundamental frequency of the building is 7.0 Hz, the mass (m1 and m2) and stiffness (k1 and k2) of the two floors of the structure are sampled as shown in Table 1, since dynamic characteristics of the auxiliary building depend on these values. Due to potential variation in the dimensions of structural components and uncertainty in their material properties, it is assumed that the distribution of mass and stiffness is normal with 10% coefficient of variation for

each variable. The damping effect of the building structure is also considered with a damping ratio (ζ_B). It is assumed that the value of ζ_B is uniformly distributed between 2% and 5%. These values are typical damping ratios for reinforced concrete and steel structures in practice (IBC, 2006).

The dynamic response of a nonstructural component, specifically the battery rack, depends on the location of the component in a building and the types of restraints. Here, it is assumed that the battery racks are fastened or fixed to each floor. The seismic response of these components is computed based on the seismic response of the corresponding floor of the building and the fundamental frequency (F_E) of the battery rack when treated as a single degree of freedom (SDOF) as shown in Fig. 1(b-c). Most types of electrical equipment in nuclear power plants are required to pass a certain level of shaking table tests for their seismic qualification. One type of such tests is the resonance test. These tests show that the fundamental frequency of most electrical equipment is in the range of 4-16Hz (Hur, 2012; Kim et al., 2012). Thus, this study assumes that the fundamental frequencies of the battery racks follow a uniform distribution from 4 to 16 Hz. These frequencies can be lower, if battery racks are not fully restrained (Hur, 2012).

2.2. Parameters for Sampling

Several properties of the structural system are considered as random variables to account for uncertainties in the simulations. They include the masses of the building floors m1 and m2, stiffnesses of each story k1 and k2, damping of the building ζ_B, fundamental frequencies of nonstructural components (F_E), and the operational capacity of nonstructural components. In order to reduce the number of MCSs, it is assumed that the masses and lateral stiffnesses of two stories are identical, respectively, and m1 = m2 and k1 = k2. Therefore, total five variables are considered including m, k, ζ_B, F_E, and the capacity. Their distributions are summarized in Table 1, which presents each variable, its unit and probabilistic distribution. Dist. stands for the probabilistic distribution, and N, U and L refer to the normal, uniform, and lognormal distribution, respectively. C.O.V. stands for the coefficient of variation. Based on the 10,000 samples of m1 = m2 and k1 = k2, the fundamental frequency of building (F_B) follows the normal distribution with the mean of 7 Hz and coefficient of variation of 7%. The fundamental frequency of nonstructural component (F_E) is 4-16 Hz, and it means that the natural period of the equipment (T_E) is 0.006 to 0.25 seconds. The operational capacity of the equipment is assumed to follow a lognormal distribution with the mean of μ and standard deviation of σ.

Table 1: Variable Parameters

		Mean	C.O.V.	Dist.*
m1 = m2	(kN*s^2/m)	25	0.1	N
k1 = k2	(kN/m)	12.8E+4	0.1	N
F_B	(Hz)	7	0.07	N
		Min	Max	Dist.*
ζ_B	(ratio)	0.02	0.05	U
F_E	(Hz)	4	16	U
T_E	(sec)	0.006	0.25	
		Mean (μ)	St.D. (σ)	Dist.*
Capacity	(g)	1.01	0.063	L

*: Dist.=Distribution; N=Normal; U=Uniform; L= Lognormal

This study focuses on the evaluation of the failure probabilities of the nonstructural components under a certain ground motion and the comparison of the results from REAK and MCS to evaluate the failure probabilities. For the estimation of the failure probabilities, 10,000 samples are generated for the conventional MCS using Latin Hypercube Sampling (LHS) technique. For the surrogate model, total of 200 samples are generated, and among them, 20 samples are used for initial training.

2.3. Ground Motion Histories

In this paper, one ground motion history is used as shown in Figure 2. The original ground motion (GM) history was recorded from the 1984 Morgan Hill Earthquake (Magnitude 6.2). For this study,

it is normalized to 1.0 g of PGA, as shown in Figure 2.

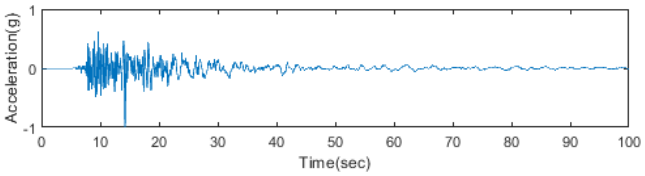

Figure 2: Scaled Ground Motion History

The spectrum acceleration of this GM is shown in Figure 3. It illustrates that the fundamental frequencies between 1 and 10 Hz have spectral accelerations larger than 1.0 g, which is the spectral acceleration of a rigid structure. It is expected to observe large values of response of building floors and nonstructural components for this ground motion.

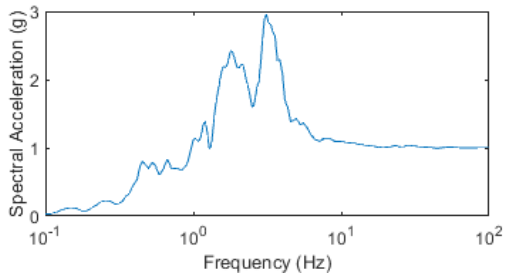

Figure 3: Spectral Acceleration

3. DYNAMIC ANALYSIS WITH A LARGE SAMPLES

3.1. Dynamic Analysis

For the selected ground motion history, the time history analysis is conducted for generated samples. For the conventional MCSs, each input variable set from 10,000 samples goes to the dynamic analysis in order to obtain the dynamic response of two floors at the locations of the equipment and the acceleration responses of the equipment by solving the following equation:

$$M\begin{Bmatrix}\ddot{u}_1\\ \ddot{u}_2\end{Bmatrix} + C\begin{Bmatrix}\dot{u}_1\\ \dot{u}_2\end{Bmatrix} + K\begin{Bmatrix}u_1\\ u_2\end{Bmatrix} = -Ml\ddot{u}_g \qquad (1)$$

where $M = \begin{bmatrix}m1 & 0\\ 0 & m2\end{bmatrix}$ is the mass matrix, $K = \begin{bmatrix}k1+k2 & -k2\\ -k2 & k2\end{bmatrix}$ is the stiffness matrix, $C = a_0M + a_0K$ is the damping matrix with $a_0 = \frac{2\zeta\omega_1\omega_2}{\omega_1+\omega_2}$ and $a_1 = \frac{2\zeta}{\omega_1+\omega_2}$.

Equation (2) is solved using the Bogachi-Shampine method (Shampine and Reichelt, 1997) which is implemented in the function, ode 23, in MATLAB (Mathworks, 2012). It is a Runge–Kutta method of order three with four stages with the First Same As Last (FSAL) property, so that it uses approximately three function evaluations per time step. The solution of Eq. (1) provides: (1) the absolute floor accelerations FA1 ($\ddot{u}_1$) and FA2 ($\ddot{u}_2$), and (2) floor displacemens FD1 (u_1) and FD2 (u_2). Using these histories of FA1 and FA2, fundamental frequencies of nonstructural components, T_E, and a constant damping ratio of 5%, acceleration response histories of these equipment are computed.

3.2. Results of the Monte Carlo Simulations

Using the simulations, the displacement and acceleration responses of building floors and nonstructural components are obtained. Among them, Figure 4 shows the absolute peak acceleration (PA) responses of equipment with respect to model parameters. In the vast majority of cases, the acceleration response of E2 located on the second floor is larger than the acceleration of E1, which is located on the first floor.

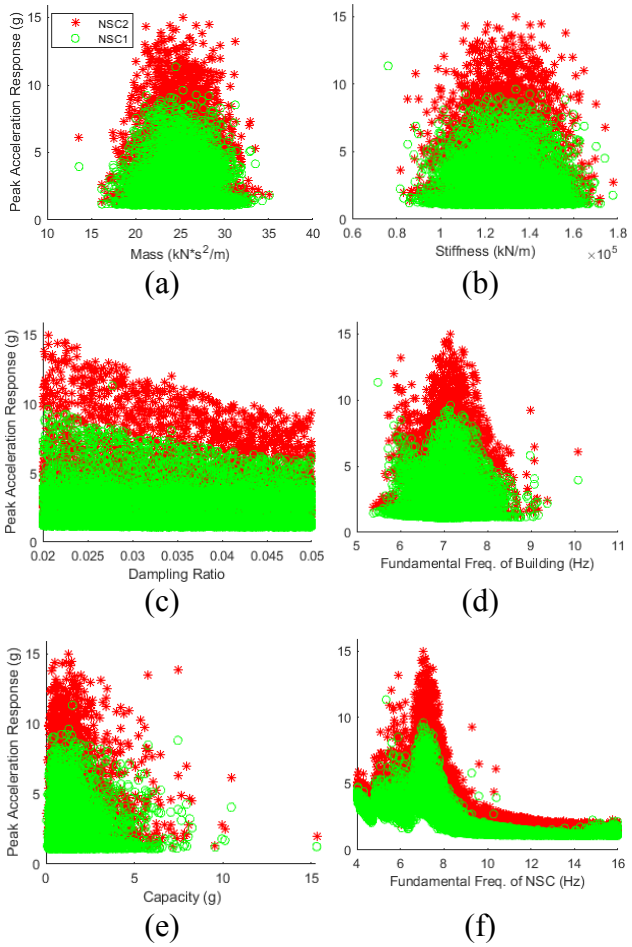

Figure 4: Analysis Result from MCSs

Depending on the mass and stiffness distributions, the acceleration response of E1 and E2 are normally distributed. Smaller values of damping ration lead to larger acceleration responses of the nonstructural component. As shown in Figure 4(f), the acceleration response of nonstructural components around the fundamental frequency of the equipment of 7 Hz is very high. This is because of the fact that this frequency coincides with the fundamental frequency of the building thus leading to resonance effects.

Another objective here is to find the rare cases where the acceleration response of E1 exceeds that of E2. It is commonly assumed that the failure of E1 contains the failure of E2, since they are correlated and the response of E2 is larger than that of E1. It is found that the seismic performance of nonstructural components located on different floors are highly correlated, and therefore the joint failure probability of E1 and E2 is very close to the failure probability of E1 (Hur et al., 2016). However, the failure probabilities and their correlation not holding true do that they must be evaluated to ensure induced errors are acceptable. Using MCSs, the rare cases where the acceleration response of E1 exceeds that of E2 can be captured with very large number of simulations. This however can be handled using surrogate models with substantially fewer number of simulations.

Table 2: Failure Probability of nonstructural components using MCS

Failure Probability of		Prob. of
E1	E2	PGA of E1 > E2
0.75	0.86	0.0097

4. SURROGATE MODELS

4.1. Algorithm of Surrogate Model

This section presents the surrogate models using adaptive Kriging-based reliability analysis method to estimate the failure probabilities of nonstructural components. This method was developed by Wang and Shafieezadeh (2018). The Kriging model $\hat{g}(x)$ can be described as follows:

$$\hat{g}(x) = F(\beta, x) + Z(x) = \beta^T f(x) + Z(x) \quad (2)$$

where $F(\beta, x)$ is the deterministic regression part representing the Kriging trend and $Z(x)$ is the Gaussian process-based stochastic interpolation. Expanding the first term $F(\beta, x)$, $f(x)$ is the Kriging basis and β is the regression coefficient of $f(x)$. $\beta^T f(x)$ has the ordinary (β_0), linear ($\beta_0 + \sum_{i=1}^{N} \beta_i x_i$), quadratic ($\beta_0 + \sum_{i=1}^{N} \beta_i x_i + \sum_{i=1}^{N} \sum_{j=i}^{N} \beta_{ij} x_i x_j$) and polynomial forms, where N is the dimension of the random input vector x. In this paper, quadratic trend function is used. Moreover, $Z(x)$ follows a stationary normal Gaussian process with zero mean and covariance matrix as shown below:

$$\mathrm{COV}\left(Z(x_i), Z(x_j)\right) = \sigma^2 R(x_i, x_j; \theta) \quad (3)$$

where σ^2 is the variance or the generalized mean square error of regression, x_i and x_j are two observations, and $R(x_i, x_j; \theta)$ is the correlation function or the so-called kernel function, which represents the correlation function of the process with hyper-parameter θ. Forms of linear, exponential, Gaussian, and Matérn functions are widely used. In this paper, the Gaussian kernel function is used with the following form:

$$R(x_i, x_j; \theta) = \prod_{k=1}^{N} \exp\left(-\theta^k \left(x_i^k - x_j^k\right)^2\right) \quad (4)$$

where N is the dimension of the random input vector. The hyper-parameter θ can be estimated via Maximum Likelihood Estimation (MLE). Feasible θ_i is explored in $(0,10)$ through the MLE. The Maximum Likelihood Estimation can be represented as

$$\theta = \underset{\theta^*}{\operatorname{argmin}} \left(\left| R(x_i, x_j; \theta) \right|^{\frac{1}{m}} \sigma^2 \right) \quad (5)$$

The regression coefficient β, and Kriging estimated mean and variance can be determined as follows:

$$\beta = (F^T R^{-1} F)^{-1} F^T R^{-1} Y$$

$$\mu_{\hat{g}}(x) = f^T(x)\beta + r^T(x) R^{-1}(y - F\beta)$$

$$\sigma_{\hat{g}}^2(x) = \sigma^2 \begin{pmatrix} 1 - r^T(x) R^{-1} r(x) \\ + \left(F^T R^{-1} r(x) - f(x)\right)^T \\ (F^T R^{-1} F)^{-1} (F^T R^{-1} r(x) - f(x)) \end{pmatrix} (6)$$

where F is the matrix of the basis function $f(x)$ evaluated at known training points, i.e. $F_{ij} = f_j(x_i)$, $i = 1, 2, \ldots, m$; $j = 1, 2, \ldots, p$, $r(x)$ is the vector of correlation between known training points x_i and an unknown point x : $r_i = R(x, x_i, \theta)$, $i = 1,2 \ldots m$, and R is the autocorrelation matrix for known training points: $R_{ij} = R(x_i, x_j, \theta)$, $i = 1,2, \ldots, m; j = 1,2, \ldots, m$. Due to the prior assumption of Kriging model, the responses from Kriging follow a normal distribution with Kriging mean $\mu_{\hat{g}}(x)$ and Kriging variance $\sigma_{\hat{g}}^2(x)$:

$$\hat{g}(x) \sim N\left(\mu_{\hat{g}}(x), \sigma_{\hat{g}}^2(x)\right) \quad (7)$$

The process of Kriging-based reliability analysis method is shown in the Algorithm below.

Table 3: Algorithm of Adaptive Kriging-based Reliability Analysis

1. Draw candidate design samples $\boldsymbol{x}_s$ and initial training samples, $\boldsymbol{x}_{tr}$, with Latin Hypercube Sampling technique (LHS)
2. Estimate the responses of training samples according to the performance function g
3. Construct the Kriging model $\hat{g}$ according to training points
4. Estimate the $\mu_{\hat{g}}(\boldsymbol{x}_s)$, $\sigma_{\hat{g}}^2(\boldsymbol{x}_s)$ and probability of $\hat{P}_f^{MCS}$ based on the surrogate model $\hat{g}$ with MCS
5. Check if the stopping criterion (specified relative error level) is satisfied or not:
   (a) Satisfied. Go to step 6.
   (b) Unsatisfied. Find the next best training point $\boldsymbol{x}_{tr}^*$ and go back to Step 2.
6. Output $\hat{P}_f^{MCS}$

4.2. Analysis Result by Surrogate Models

For the surrogate models, the same distributions of variables are used, but the number of simulations are drastically reduced compared to the MCS. In order to estimate the failure probabilities of E1 and E2 and the probability that the acceleration response of E1 exceeds that of E2, three surrogate models are trained and *P*(failure of E1), P(failure of E2), and P(Acceleration of E1 is larger than that of E2) are derived subsequently. 20 samples are initially

used for training and about 180 additional samples are generated adaptively to further train the Kriging model. The analysis results are shown in Table 4 below. It can be observed that and they are very close to the result obtained by MCSs.

Table 4: Failure Probability of nonstructural components using Surrogate Models

Failure Probability of E1	E2	Probability of PA response E1 > E2
0.76	0.86	0.011

5. COMPARISON OF TWO METHODS

This study shows the computational efficiency and accuracy of the surrogate model in the uncertainty analysis comparing to the conventional MCSs. For the comparison, three probabilities were estimated as shown in Figures 5 and 6. In order to find the rare cases that the acceleration response of E1 exceeds that of E2, total 10,000 sample sets are simulated, and among them, 97 cases were observed to satisfy this condition. Therefore, the probability of that event is about 1%. On the other hand, the surrogate models were trained about 200 times adaptively. Evaluated failure probabilities of E1 and E2 are shown in Figure 6. It is observed that the surrogate model-based reliability analysis is able to achieve high accuracy with 5% relative error.

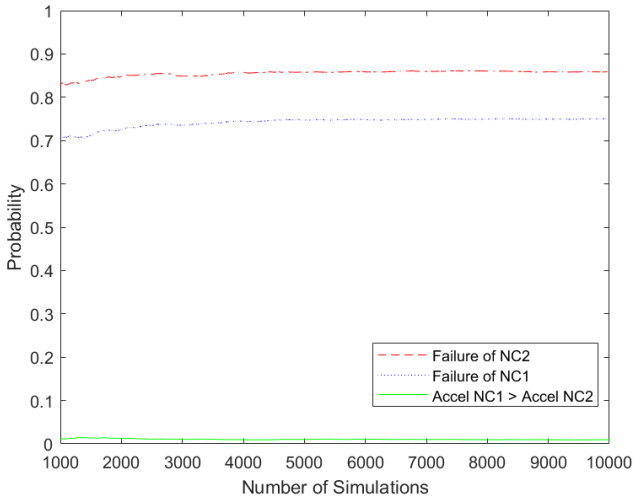

Figure 5: Failure Probabilities using MCS

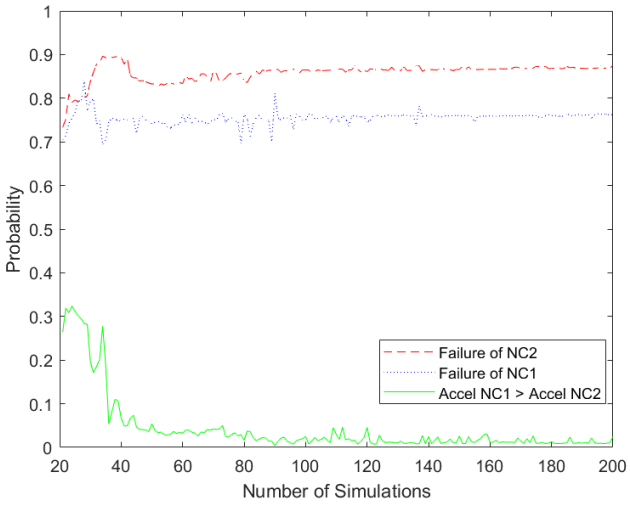

Figure 6: Failure Probabilities using Surrogate Models

6. CONCLUSIONS

This study evaluated the operational failure probabilities of identical nonstructural components mounted on two different floors of an auxiliary building in a pseudo-plant subjected to seismic shakings. Uncertainties in the dynamic features of auxiliary buildings and nonstructural components were characterized using a set of random variables. With these variables, a large number of samples were generated using Latin Hypercube Sampling (LHS) method. For each set of samples, a time history analysis was performed with a selected ground motion history, and the seismic performance of nonstructural components was evaluated. These seismic performances were compared to the probabilistic seismic capacity of the equipment, and the failure probabilities were estimated. Moreover, the probability that the acceleration response of E1 exceeds that of E2 was estimated, which has been commonly neglected for the seismic analysis of nonstructural components. These probabilities by the MCSs were compared to those by the surrogate models. It was found that surrogate models are computationally very efficient for the evaluation of the failure probability of any components. In order to evaluate the cases that the acceleration response of E1 exceeds that of E2, the surrogate

modeling approach was very efficient even though the probability of that event is very small (around 1%).

It should be noted that the large failure probability obtained in our reliability analysis for nonstructural components is expected only for a nuclear power plant subjected to earthquakes of magnitude much greater than the design basis. Because the seismic design basis for equipment assures a high confidence of a low probability of failure, the associated failure probability at earthquakes near the design basis level must be small. Moreover, the Monte Carlo analysis did enable the assessment of the effect of correlation on the joint failure probability of nonstructural components. The results indicated that greater consideration may be warranted in assessing the degree of correlation between the failure probabilities of components located at different areas of a building.

7. REFERENCES

Y. Kitada, T. Hirotani And M. Iguchi, "Models Test on Dynamic Structure-Structure Interaction of Nuclear Power Plant Buildings," *Nuclear Engineering and Design*, Vol. 192, pp 205-236, (1999).

B. Ellingwood, Bruce R. "Issues related to structural aging in probabilistic risk assessment of nuclear power plants." *Reliability Engineering & System Safety62.3* (1998): 171-183

NUREG - U.S.Nuclear Regulatory Commission, "Seismic Fragility of Nuclear Power Plant Components [PHASE II]," NUREG/CR-4659, BNL-NUREG-52007, Vol. 2-4, Department of Nuclear Energy, Brookhaven National Laboratory, Long Island, NY(1987)

J. Hur "Seismic performance evaluation of switch-board cabinets using nonlinear numerical models." (2012). Georgia Institute of Technology, Atlanta, GA

IBC, ICC. "International building code." International Code Council, Inc.(formerly BOCA, ICBO and SBCCI) 4051: 60478-5795 (2006).

Kim, Min Kyu, In-Kil Choi, and Jeong-Moon Seo. "A shaking table test for an evaluation of seismic behavior of 480V MCC." *Nuclear Engineering and Design,* 243: 341-355 (2012)

Shampine, L.F. and Reichelt, M.W., The Matlab ODE Suite, *SIAM Journal on Scientific Computing* 18 (1): 1–22 (1997)

Mathworks, "Bioinformatics Toolbox: User's Guide" The MathWorks, Inc. R2012a (2012)

Hur, J., Guler, A., Sezen, H., Aldemir, T., & Denning, R., (2016), "Assessment of conservatism in the separation of variables approach to seismic probabilistic risk assessment", Proceedings of *The International Congress on Advances in Nuclear Power Plants (ICAPP)*, San Francisco, CA, April 17-20, 2016.